Proceedings Paper:
Bandyopadhyay, A, Bertling, K, Garg, D et al. (10 more authors) (2021) Sub-surface damage detection in marble structures using THz time domain and laser feedback interferometric imaging. In: Proceedings of SPIE - The International Society for Optical Engineering. SPIE OPTICAL METROLOGY, 21-26 Jun 2021, Online. SPIE . ISBN 9781510644021

https://doi.org/10.1117/12.2592548

Sub-surface damage detection in marble structures using THz time domain and laser feedback interferometric imaging

Bandyopadhyay, Aparajita, Bertling, Karl, Garg, Diksha, Singh, Khushboo, Gillespie, Tim, et al.

Aparajita Bandyopadhyay, Karl Bertling, Diksha Garg, Khushboo Singh, Tim Gillespie, Yah Leng Lim, Lianhe Li, Paul Dean, Dragan Indjin, Edmund H. Linfield, A. Giles Davies, Aleksandar D. Rakic, Amartya Sengupta, "Sub-surface damage detection in marble structures using THz time domain and laser feedback interferometric imaging," Proc. SPIE 11784, Optics for Arts, Architecture, and Archaeology VIII, 117840T (8 July 2021); doi: 10.1117/12.2592548

SPIE.

Event: SPIE Optical Metrology, 2021, Online Only

Sub-surface damage detection in marble structures using THz time domain and laser feedback interferometric imaging

Aparajita Bandyopadhyay[a], Karl Bertling[b], Diksha Garg[c], Khushboo Singh[c], Tim Gillespie[b], Yah Leng Lim[b], Lianhe Li[d], Paul Dean[d], Dragan Indjin[d], Edmund H. Linfield[d], A. Giles Davies[d], Aleksandar D. Rakic[b,*] and Amartya Sengupta[b,c,†]

[a]Joint Advanced Technology Center-IIT Delhi, Delhi 110016, India; [b]School of Information Technology & Electrical Engineering, The University of Queensland, St Lucia QLD 4072, Australia; [c]Department of Physics, Indian Institute of Technology, Delhi 110016, India; [d]School of Electronic and Electrical Engineering, University of Leeds, Leeds LS2 9JT UK

ABSTRACT

This present collaborative research, undertaken in two different hemispheres, in an effort to address the challenge of early structural and sub-surface assessment of heritage marble architectures, like the Taj Mahal, using two complementary non-contact, non-invasive imaging techniques in the THz spectral range. In our previous work, it was already demonstrated that the complementary techniques of broadband Terahertz Time Domain Imaging (THz-TDI) and micro-Raman spectroscopy are successful in probing volume and surface damage in marble with *Pietra-dura* work. In the present work, the unique combination of THz-TDI and highly sensitive THz-Laser Feedback Interferometry (THz-LFI) have been explored to study sub-surface damage and irregularities of marble structures with *Pietra-dura* motif. These optical techniques hold immense possibility in large-scale architectural restoration projects as they collectively provide accurate structural depth profile up to several inches into the volume of the marble including the strain generated within the structure leading to potential cracks.

Keywords: Terahertz, time domain imaging, spectroscopic imaging, THz-laser feedback interferometry, quantum cascade laser, sub-surface damage, marble, Taj Mahal

1. INTRODUCTION

Built in the 17th century by the emperor Shah Jahan in the memory of his queen, Mumtaz Mahal, the Taj Mahal is an architectural wonder in white marble with its exquisite inlay works. Famously known as the 'monument of love' worldwide, it continues to draw visitors despite the current difficult time after the longest closure due to the lockdown [1]. Perhaps unknown to most of her patrons, however, this marvelous structure is suffering from critical structural damage caused by her tilt towards the bank of the river Yamuna [2]. Exhaustive damage assessment and required restoration of this structure is already underway; however, the traditional means of structural survey in heritage architectures, like the Taj Mahal, is arduous and subjective and in most cases yield positive detection only after the damages become visually apparent. The undetected sub-surface strain and the propagation of cracks in such structures, however, could lead to a complicated, costly, and long-drawn restoration procedures which ultimately might prove to be too little too late. To address this aspect of sub-surface damage detection in these marble structures, here we have introduced a combination of through-marble imaging techniques, namely, the broadband Terahertz Time Domain Imaging (THz-TDI) covering the range of 0 – 4 THz and highly sensitive THz-Laser Feedback Interferometry (THz-LFI) around 2.7 THz. In our previous work [3], we have already observed that THz range, indeed, has large penetration depth inside the marble structures and can sense water damage as well as surface and sub-surface cracks. This present combination of two complementary techniques, however, could further these observation as it would permit a complete mapping of the sub-surface profiles in terms of depth and spatial resolution of any cracks, propagation of cracks and even the points of acute strain in the structure leading to potential cracks.

* Corresponding Author 1 contact information: a.rakic@uq.edu.au
† Corresponding Author 2 contact information: amartya@physics.iitd.ac.in, +91 11 2659 1382

Optics for Arts, Architecture, and Archaeology VIII, edited by Haida Liang, Roger Groves, Proc. of SPIE
Vol. 11784, 117840T · © 2021 SPIE · CCC code: 0277-786X/21/$21 · doi: 10.1117/12.2592548

Representative marble slabs of thickness ranging from several millimeters to few tens of millimeters with stone inlay motifs on the surface have been employed in our present experimental imaging studies. Since both the techniques could directly measure both amplitude and phase, a depth resolved series of time-of-flight THz images provide surface morphology, the underlaying design impression made by the artists for the stone inlay works as well as the slippage and the cracks in the volume of the marble. Most importantly, however, we could observe a network of crystalline grain boundaries in the volume of the marble, visible due to the strong scattering absorption triggered because of our probing wavelengths around hundreds of microns coinciding with the natural grain boundaries of the marble. These obtained 'tomographic' images from the depth of the marble, essentially could establish future pathways for an objective assessment of sub-surface damages, even at an asymptomatic level, and would ensure greater success in the conservation efforts of spectacular marble structures, like Taj Mahal.

2. TERAHERTZ TIME DOMAIN IMAGING

2.1 THz-TDI leading to spectroscopic imaging

The THz-TDI technique, as a non-contact and non-invasive tool has been used in widespread applications ranging from medical diagnostics and biological studies, security screening, material characterization, quality control and more recently, culture and/or heritage conservation [4]. To implement this spectroscopic imaging technique, an object is imaged with a broadband THz source over a range of THz frequencies and the transmitted or reflected signal off the object is recorded through gated coherent detection. This ensures direct measurement of the THz electric field with both amplitude and phase information. When this THz spectroscopic information is collected over a certain range of two-dimensional spatial coordinates of that object and its surroundings, the resulting composite multidimensional array in three-dimensions represents an image where each pixel corresponds to a physical location of the object under study while the third dimension carries the THz spectral information of that location over a certain frequency band. In simple terms, THz spectral image of an object is essentially a 2-D THz spectral map which can be obtained by proper Fourier deconvolution from the experimentally obtained time-domain image gathered through gated coherent detection.

Especially in the case of heritage conservation where the object of interest could be shrouded under composite barriers, such as, a sarcophagus or Fresco [5]; or the object itself could have several layers, such as, an old manuscript or painting [6], this type of THz imaging is increasingly being employed. Apart from sub-surface information, most of the typical chemical substances, such as, ink, dye, glue, glaze, metal oxides etc., found in these heritage objects have characteristic THz spectroscopic signatures [7]. The time domain signal acquisition with low frequency components (less than 1.5 THz), ensure greater penetrability through dielectric layers; while the time-of-flight information of each femtosecond THz pulse in such acquisition, provides the information of various layers under study. This strategy of using the lower frequency band, however, suffers from compromised spatial resolution of features of interest and thus to gather a rather complete profile, it is essential that an object be probed both through lower and higher frequency components.

2.2 THz-TDI experimental Setup

In the current study, photoconductive antenna-based THz-TDS (TERAFLASH®, TOPTICA Photonics AG) system with dynamic range of 90 dB @ 0.5 THz with bandwidth up to 5.5 THz was used. This was integrated with a computer-controlled raster scanner working in both linear transmission and reflection configuration with 8° angle of incidence/reflection [8]. All experiments are performed in controlled environment with $T = 21 \pm 2°$ and relative humidity of 42 ± 5 %. To perform THz TDI, representative marble coasters of thickness 3 mm with Pietra Dura motifs on the surface (obtained from Central Cottage Industries Emporium, New Delhi, India) were used. The composite THz image in time domain was obtained with a scan range of 100 ps and sampling interval of 0.05 ps, averaged over 6 pulse traces at each coordinate with either 0.2 mm or 0.5 mm stage movement in each X and Y directions, which takes approximately 1 second per pixel point including the stage movement. For transmission spectroscopic measurements, the data was collected with the same time domain scanning setting over 8000 averages which takes approximately 12 minutes.

2.3 THz Spectroscopic and Imaging results

The result of THz transmission measurement is given in Figure 1 where the black line corresponds to the THz-TDS reference and the lines in 10 different colours represent the time domain signal through 10 randomly selected points without any inlay motifs through the 3 mm thick marble coaster. These THz pulses through the marble are also shown separately in the top inset graph. From this figure, we notice that the time delay of the reference pulse and the transmitted pulse through the marble is ~ 42.5 ps which signifies a broadband optical refractive index of 4.25 for this marble coaster.

Additionally, we notice that the average transmitted THz amplitude through these 10 points is about 20% of the reference THz amplitude through air. These high values of both real and imaginary parts of the complex refractive index of the marble could be attributed to the very nature of the marble structure rather than the material $CaCO_3$. Both under visual and microscopic inspection, we find polycrystalline nature of the marble with grain boundaries varying from tens of microns to the order of mm [3]. Because of this natural 'granular' composition of the marble structure THz radiation undergoes very strong Mie scattering in forward direction during the transmission, resulting in substantially high value of the complex refractive index [9]. This fact also suggests that higher frequency components of THz pulse will suffer significant attenuation and the transmitted THz amplitude is the result of principally the low frequency components expected to be having greater penetrability through the marble polycrystalline structure.

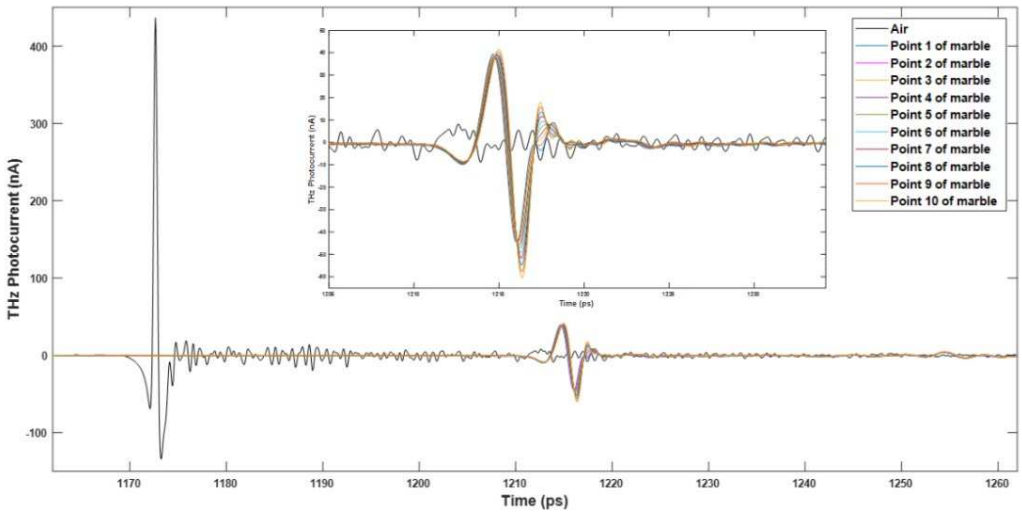

Figure 1. Time domain THz transmission through marble coaster with orange flower motif and through air as the reference. *Top Inset:* THz pulse transmission through 10 randomly chosen points on the marble coaster without any inlay motif.

An intentional hairline crack, of thickness of ~ 120 μm, was also introduced [3] at one side of the coaster as shown in the left-hand corner inset of Figure 2. THz time domain transmission signals collected through the air, average signal through marble over the 10 points and through the crack are Fourier transformed to obtain the spectral response of the marble as shown in Figure 2 in black, blue and red solid lines, respectively. The amplitude plot clearly shows that while the system has strong spectral response even beyond 4.5 THz, the transmitted signal through the marble is limited to ~ 1.5 THz. In fact, frequency components above 300 GHz (wavelength of ~ 1 cm) suffer exponentially increasing attenuation due to the scattering from the grain boundaries as discussed above. Also, we notice that marble does not have any resonant THz absorption peaks within this range as all the 'dips' in the amplitude plots are accounted for by the water vapour lines in the THz range. At the same time, we also notice that the THz transmission through the crack is less than any other points of the marble coaster. This apparently counterintuitive observation is, however, expected; as the presence of 'crack' increases scattering interactions and multiple reflections for the THz frequency components at surface, as well as through the entire volume of the marble coaster.

Subsequent to the spectroscopic measurement, THz time-domain transmission image (of the area of the marble coaster centered around the crack in the XY plane) is obtained using raster scan technique with 0.5 mm stage movement. Using Fourier deconvolution and normalization, reconstructed intensity and phase images of the specific section of the raw time domain image are generated at specific THz frequency values. The right-hand side top inset in Figure 2 shows 4 sets of such intensity images. As expected, there is no transmission of THz radiation at 1.5 THz and beyond. However, at lower frequency values of 0.8 THz and 1.0 THz, the images clearly show the presence of the hairline crack where the transmissivity of THz goes down significantly, as shown in these false colour images where red represents very high transmission and blue represents low THz transmission.

Because of this compromised transmission of high frequency THz radiation, we employed THz-TDI technique in reflection configuration to further probe the marble coaster. The coaster was placed on a plane metal surface which was

also used the reference for THz alignment. From our transmission studies, it was also evident that for frequency components above 0.3 THz, THz radiation passing through the marble coaster without any ornamentation will suffer significant absorption through the volume of the marble and any reflection by the metal holder thereof will not be able to reach the receiver. In this reflection configuration, we obtain time domain raw image of the coaster area centered around the stalk of the orange flower motif (of an area ~ 33 × 22 mm^2) with 0.2 mm stage movement resulting in 165 × 110 pixels. Using the same analyses technique as mentioned above, reconstructed intensity and phase images at specific THz frequency values are generated in 'false' colour. In the resulting images, the red represents very high reflectivity and blue represents very low reflectivity.

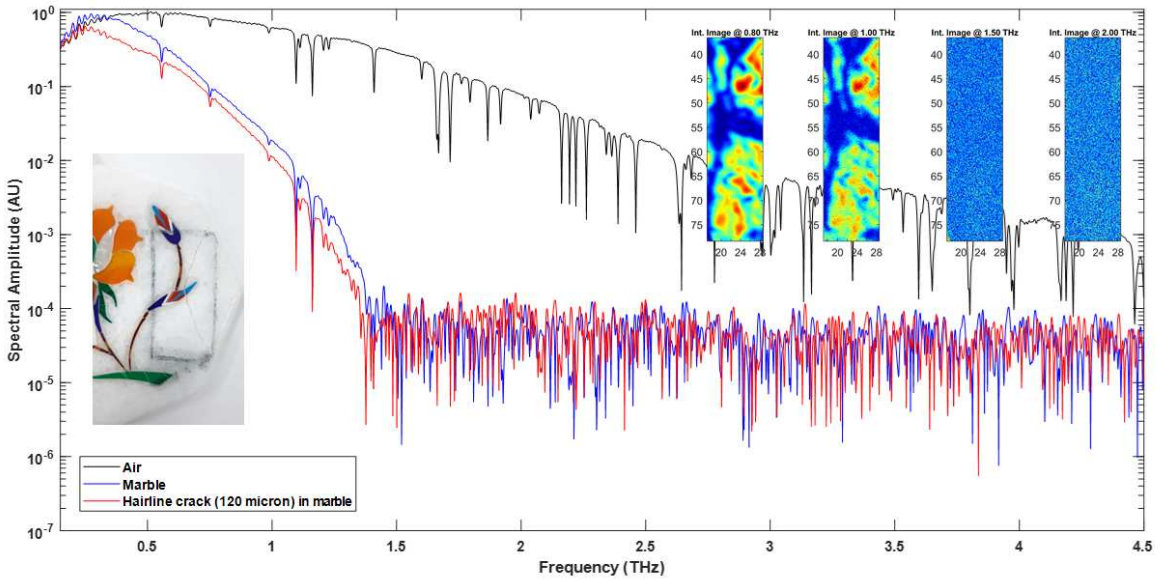

Figure 2. The spectral response of the THz transmission through the marble coaster with hairline crack. *Bottom Left-Hand Inset:* Visual image of the 'crack' on the coaster; *Top Right-Hand Inset:* Reconstructed transmission THz intensity images of the 'crack'.

In Figure 3, the reconstructed intensity images of the imaged area are shown for 8 specific frequency values, that is, for 0.8, 1.0, 1.5, 2.0, 2.2, 2.5, 2.7, 2.8 THz. As expected, the images formed at lower frequencies up to 2 THz show significantly higher reflectivity with sharp contrast as the THz source power used in the imaging set up is relatively higher for lower THz frequency components. We also notice that 'blue' regions indicate lower reflectivity in the images wherever there are any 'edges' due to diffused scattering or 'junctures' where glue is applied in the inlay work, which is highly absorbing in THz region. However, these low frequency images also suffer from low spatial resolution as expected. Beyond 2 THz, the images are formed with compromised contrast, due to reduced THz source power of the system, but with greater spatial resolution. This set of reflectivity images are also somewhat of 'tomographic' nature as the THz reflections at each specific frequency point for any set of materials present on the coaster are taking place at specific depth. This depth is the penetration depth of the radiation at that frequency for a particular material. Thus, at lower frequencies, where the penetration depth of THz radiation is high for marble, we see very high reflectivity at areas without the inlay work and very clear definition of the marble 'grain' coming from the volume of the marble. In fact, the image formed at 2 THz clearly shows this 'layered' aspect of various materials, that is, the marble base, the glue/mortar and the colourful stonework in this pseudo-tomographic image. We also notice the spectral imaging aspect of this technique which becomes apparent in higher frequency range. We observe that there is a sharp reflectivity change for the stonework materials beyond 2 THz while the reflectivity of the marble remains nominally the same. These materials used for the stonework become progressively absorbing towards higher end of the frequency values; but because of compromised dynamic range with low THz power of the THz-TDI system, images formed at or beyond 3 THz suffer from system noise (images are not shown here). Thus, probing these materials using high-power high-frequency THz imaging system becomes a necessity for any further spectral characterization.

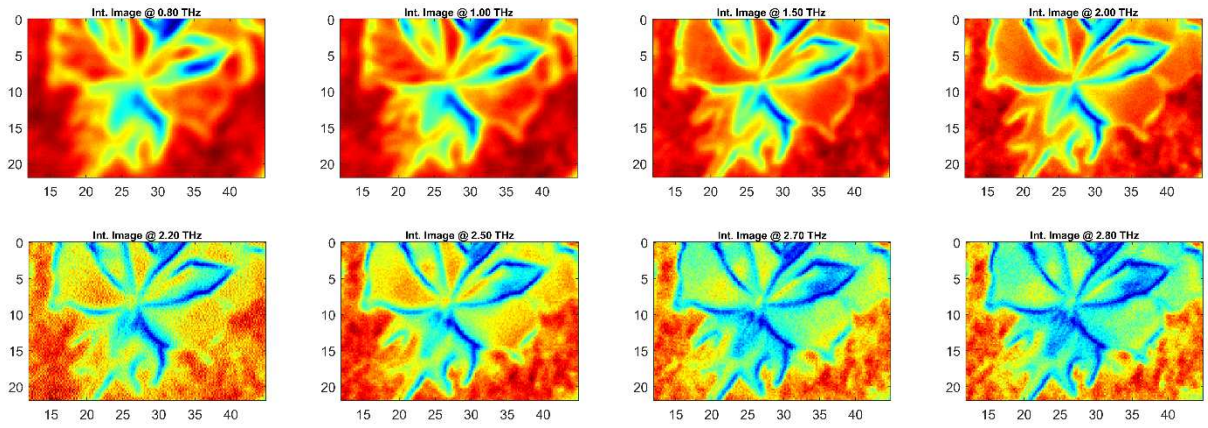

Figure 3. The THz reconstructed intensity images of the marble coaster with orange flower motif in reflection configuration at 0.8, 1.0, 1.5, 2.0, 2.2, 2.5, 2.7, 2.8 THz.

In Figure 4, the reconstructed phase images of the imaged area are shown for the same 8 specific frequency values, that is, for 0.8, 1.0, 1.5, 2.0, 2.2, 2.5, 2.7, 2.8 THz. In these phase images, at lower THz frequencies where appreciable penetration of THz radiation takes place within the marble, we notice that considerable phase accumulation occurs, which is represented by red in the 'false' colour image. However, this phase accumulation is not regular over any spatial scale which is expected because of the strong scattering interactions within the marble volume destroying the uniform phase information carried by the THz pulse. With increasing frequencies, or in other words, decreasing penetration depth, phase accumulation decreases, and the phase images tend to lose contrast between the marble and the inlay works. The exception remains, however, specifically at the area of the 'green stalk' of the orange flower motif. This area even at 2 THz shows sustained phase accumulation suggesting that the 'green stalk' stonework material to be slightly more dielectric (or in other words having lower attenuation in THz range) in nature but having significantly high real part of refractive index. Because of these reasons, the phase accumulation even at higher frequency with very limited penetration depth produces significant contrast at 2 THz. Also, in phase images of 2, 2.2 and 2.5 THz, we again observe clear sign of spectroscopic imaging in action where the 'orange petal', 'silver petal' and the 'green stalk' of the stonework flower motif, all show different 'colours' in the phase images. Unfortunately, however, at higher frequencies we failed to observe these material specific phase dynamics due to lack of source strength as discussed above.

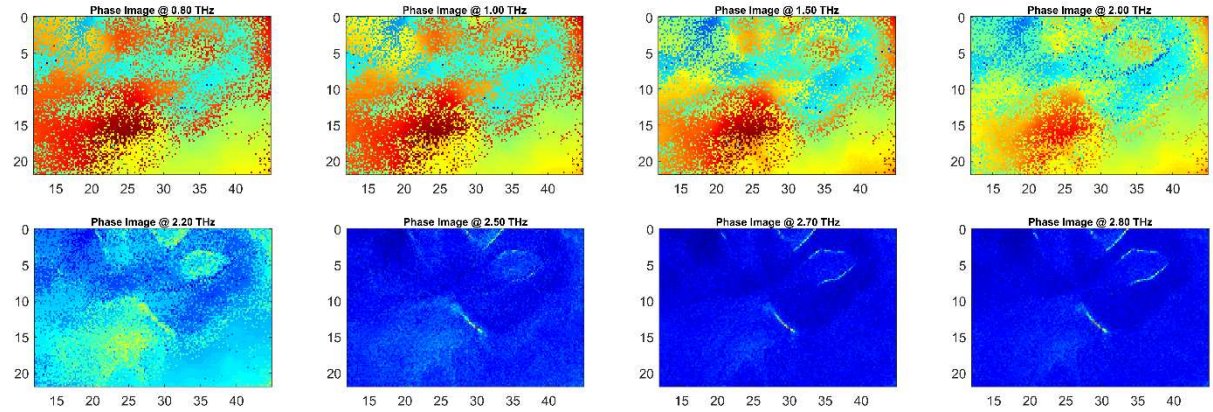

Figure 4. The THz reconstructed phase images of the marble coaster with orange flower motif in reflection configuration at 0.8, 1.0, 1.5, 2.0, 2.2, 2.5, 2.7, 2.8 THz.

3. THZ-LASER FEEDBACK INTERFEROMETRY

3.1 Laser Feedback Interferometry with Terahertz Quantum Cascade Lasers

The use of Laser Feedback Interferometry (LFI) with THz Quantum cascade lasers (QCL) is a powerful combination which not only exploits the high emitted power of the QCL as a source but utilizes a self-detection scheme (where QCL is both the source and the detector), which inherently suppresses background radiation (separating background radiation from desired signal is a common problem with many external THz detectors) while taking advantage of the coherent nature of the source [10]. Due to the source also being the detector LFI systems tend to be compact, self-aligned, with potential for high sensitivity [11] making them ideal for interferometric imaging (providing both amplitude and phase information from a target [12]) and with appropriate calibration can be used to extract complex optical properties of a target [13-15]. Pulsing the QCL in such a system allows for higher operating temperatures and higher output powers along with the potential for high-speed imaging [16-18].

The implementation used here relies on the THz QCL to be pulsed with a large-current square pulse with a slight current ramp. This small ramp induces a small sweep on the operating frequency. Ultimately this results in a series of interferometric fringes (see Fig. 5) which can be monitored via the changes in laser terminal voltage. The number of fringes is based on the size of the induced frequency sweep and the distance to the target; however, the amplitude and phase (position of peaks in time domain) are more directly related to the target itself. The amplitude of the fringes is directly related to the reflectivity of the target under interrogation (the reflectivity can change due a change in material as the beam is scanned or a change in the angle between the surface and the optical axis of the interrogation beam. The phase (position of the peaks in the time domain) is a result of either a change in lateral surface profile (a small distance change with a complete phase cycle/fringe shift covered by a lambda/2 change) or a change in material with change in phase-shift on reflection. By scanning the beam and collecting interferograms over a number of points across the target surface, amplitude and phase mapping/image of the target can be constructed. An easy way to extract this information from the interferogram is to use a Fast Fourier transform (FFT) and utilise the frequency bin corresponding to the frequency of the interferometric fringes for both the amplitude (real) and phase (imaginary) information.

3.2 LFI experimental Setup

The experimental setup is shown in Figure 5. The QCL used consisted of a 12 μm-thick GaAs/AlGaAs 9-well phonon-assisted active region with a design frequency of ~2.9 - 3.2 THz [19]. The active region layer structure starting from the injection barrier was **4**/10.1/**0.5**/16.2/**1**/12.9/**2**/11.8/**3**/9.5/**3**/8.6/**3**/7.1/**3**/17/**3**/14.5 nm. The structure was grown by solid-source molecular beam epitaxy on a semi-insulating GaAs substrate, with the active region grown between doped upper 50 nm-thick ($n = 5 \times 10^{18}$ cm^{-3}) and lower 700 nm thick ($n = 2 \times 10^{18}$ cm^{-3}) GaAs contact layers. The wafer was processed into 150 μm wide surface-plasmon ridge waveguide structures using photolithography and wet chemical etching, with the substrate thinned to ~200 μm. The device was then mechanically cleaved to define a ridge of length 2 mm. The actual emission frequency was 2.71 THz measured via the process described here [20].

The QCL was mounted the cold finger of a mechanical Stirling cryocooler (Cryotel GT, Sunpower, Inc.) via a custom-built copper T-piece with integrated electronics for electrical matching, delivery and recover of the laser drive pulse. This was connected via custom flex transmission line to a custom build laser pulse transceiver which both supplied the laser pulse, performed signal condition, recovered and digitized the LFI interfergram and extracted the amplitude and phase information (via FFT). Details of the details of the drive electronics and signal conditioning can be seen in Ref. [17].

The Stirling cooler operated at 50 K (selected to maximize the combination of the laser output power, frequency sweep and temperature stability). The laser was pulsed at 600 ns with a 33% duty cycle and a laser current between 1.1 A to 0.9 A (200 mA negative current ramp). The output beam was collimated with a 30 mm focal length Tsurupica plastic lens (25 mm clear aperture, Tsurupica-RR-CX-1-30-SPS, Broadband, Inc.) and the focusing (objective) lens of 50 mm focal length lens (30 mm clear aperture, Tsurupica-RR-CX-1.5-50-SPS, Broadband, Inc.), with the total path length between the QCL and the target being of 1.6 m. The lateral resolution of the system (based on the modulation transfer function measurements carried out on the 1951 US air force resolution target) is approximately 130 μm.

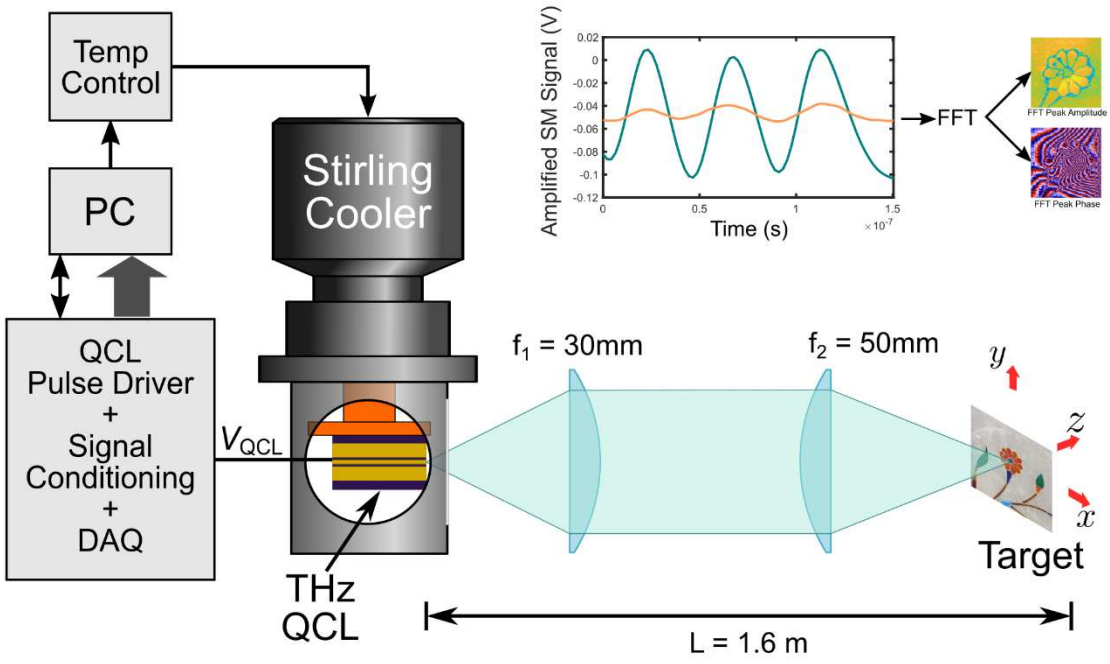

Figure 5. Schematic Diagram of the experimental setup. *Top Right:* Example of typical LFI interferograms captured by the system with a FFT used to separate the amplitude and phase information.

3.3 LFI Imaging results

Figure 6 shows the results of a 301 × 301 pixel scan with each pixel representing the THz reflection from a 50 × 50 μm^2 area of the marble coaster with a small inlaid flower. The image has strong contrast between the marble structure, the inlay and the mortar holding the inlay in both the THz amplitude and phase images. The marble has a distinct fine grain which is obvious in the THz amplitude image and the mortar show a large granular quality composite of filling material and gluing agent. More interesting is the structures which appears in both THz images but are not obvious in the photograph. These include distinct lines (horizontal and slanted towards the vertical) in the petals at about 3 and 5 o'clock respectively. There are also small areas of reduced reflectivity and phase change in the marble in bottom right corner which could be attributed to the sub surface air pockets or defects.

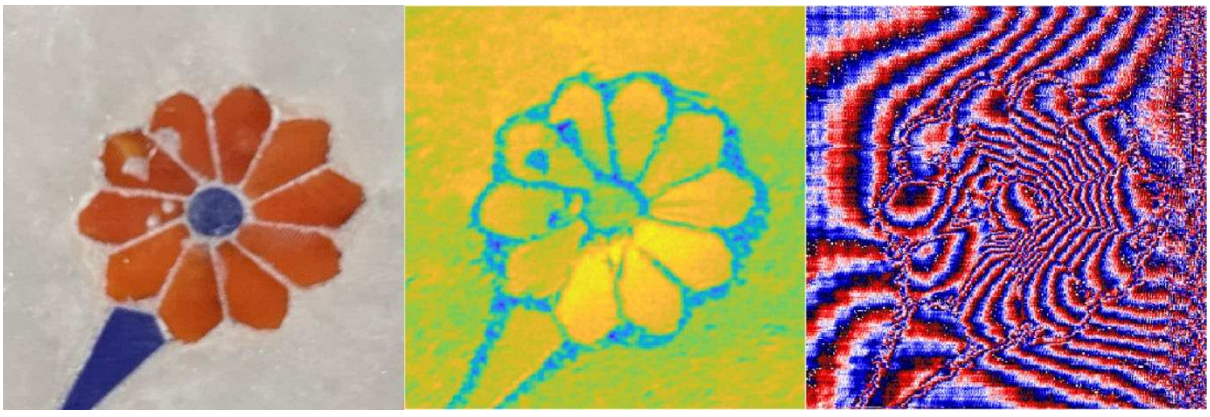

Figure 6. *Left:* Photo of inlay on the marble coaster. *Center:* Corresponding THz Amplitude LFI image. *Right:* Corresponding THZ Phase LFI Image.

These THz images were obtained, both in amplitude and phase, at 2.7 THz have very sharp contrast because of higher THz power as opposed to THz-TDI experiment where the source power is very low at this specific frequency mark. The

sub-surface irregularities are also captured with very high spatial resolution: the phase image could further capture the underlying strain generated in the marble structure during the process of the inlaid work. However, because of the limited penetration depth of THz radiation at this high frequency, which is expected to be in the order of 100 μm, these sub-surface structural irregularities and strain captured in the above images are very close to the surface.

4. CONCLUSIONS

4.1 Sub-surface damage detection using THz imaging

In summary, we could show the usability of THz-TDI technique in detecting sub-surface crack propagation and crystalline structure, especially in lower frequency components through several millimeters of marble. However, at higher frequencies, both THz-TDI and THz-LFI could show sub-surface irregularities in marble and inlay works which are not visually apparent but lie hundreds of microns below the true surface. Additionally, THz-LFI technique at 2.7 THz could also produce phase images which could sense the built-up strain in the marble structure due to the inlay work itself. In future, we would like to extend this study to the actual stone sample obtained from the Taj Mahal directly and advance towards a dual-platform non-contact, non-invasive imaging setup to help the conservation and restoration initiative of the Taj Mahal or other heritage structures of the world.

4.2 Application of complementary techniques leading to newer perspectives

Beyond the intended objective of sub-surface damage detection, the current study also unraveled unique spectral profiles of the materials used in this representative marble coaster with *Pietra-Dura* work. Using THz-TDI technique and advanced image processing techniques we could observe these spectral dynamics at higher THz frequencies; however, due to limited source power, these high frequency images show compromised contrast. On the other hand, using the complementary technique of THz-LFI at 2.7 THz, we could capture the very vivid intensity and phase images of the coaster. Thus, in future this technique using several distinct THz-QCL sources could produce high frequency differential spectroscopic images where this spectral dynamics of different mineralogical materials in THz range could be highlighted.

ACKNOWLEDGEMENTS AND CONTRIBUTIONS

Funding agencies: THz-TDI part of this work is partly sponsored by (a) Defence Research and Development Organization (DRDO) vide Grant # DFTM/03/3203/M/01/JATC, and (b) the Department of Atomic Energy - Board of Research in Nuclear Sciences (DAE-BRNS) vide Grant # 37(3)/14/01/2016-BRNS/37015. THz-LFI work acknowledges support from: the Australian Research Council Discovery Project (DP200101948, DP210103342); and the Engineering and Physical Sciences Research Council (EPSRC UK) (EP/J002356/1, EP/P021859/1, and EP/T034246/1).

Author Contributions: DG and KS have been responsible for THz-TDI system alignment, sample and data collection; AB has done the THz-TDI analysis, prepared the graphics and the manuscript; KB designed and performed and analyzed the THz-LFI experiments. YL, TG, KB and ADR developed and build the THz-LFI system. PD, LHL, DI, EHL, and AGD developed and fabricated the THz QCL. AS is responsible for providing THz-TDI facility management, overall supervision and has extensively reviewed the manuscript. All authors have seen and commented on the manuscript.

Data Availability: Data underlying the results presented in this manuscript are not publicly available at this time but may be obtained from the corresponding author upon reasonable request.

REFERENCES

[1] https://www.indiatoday.in/cities/agra/story/tourism-industry-agra-taj-mahal-coronavirus-1780948-2021-03-19 Retrieved on May 27, 2021.

[2] https://www.bbc.co.uk/news/resources/idt-sh/twilight_of_the_taj Retrieved on May 27, 2021.

[3] Aparajita Bandyopadhyay, Diksha Garg, Amartya Sengupta. “Micro-Raman spectroscopy and THz time domain spectroscopic imaging of Pietra Dura marble inlay work resembling Taj Mahal architectural motifs”. Proc. SPIE **11058**, Optics for Arts, Architecture, and Archaeology VII, 1105819 (2019).

[4] Aparajita Bandyopadhyay & Amartya Sengupta. “A Review of the Concept, Applications and Implementation Issues of Terahertz Spectral Imaging Technique”. IETE Technical Review (2021).

[5] Eva-Maria Stübling, Arno Rehn, Tabea Siebrecht, Yannick Bauckhage, Lena Öhrström, Patrick Eppenberger, Jan C. Balzer, Frank Rühli, Martin Koch. Application of a robotic THz imaging system for sub-surface analysis of ancient human remains. Sci Rep **9**, 3390 (2019).

[6] Corinna L. K. Dandolo, Gilda M. P. Saldaña, Mirta A. I. Caballero, Monserrat A. G. Sepúlveda, Arturo I. Hernández-Serrano, Alejandro M. Orozco, Joselyn A. Calderón, Melba S. C. Zárate, Karen L. González, Eunice C. P. de Dios, Gerardo H. Rosales, Enrique Castro-Camus. Terahertz Time-Domain Imaging to Guide a Conservation Intervention on a Stratified Easel Painting. J Infrared Milli Terahz Waves **39**, 773–784 (2018).

[7] Antonino Cosentino. “Terahertz and Cultural Heritage Science: Examination of Art and Archaeology”. Technologies **4**, 6-19 (2016).

[8] Diksha Garg, Aparajita Bandyopadhyay, and Amartya Sengupta, "Measurement of moisture content in milk powder using terahertz time-domain spectroscopy", Proc. SPIE **11685**, Terahertz, RF, Millimeter, and Submillimeter-Wave Technology and Applications XIV, 1168516 (2021)

[9] Aparajita Bandyopadhyay, Amartya Sengupta, Robert B. Barat, Dale E. Gary, John F. Federici, Minghan Chen and David B. Tanner. “Effects of Scattering on THz Spectra of Granular Solids”. Int J Infrared Milli Waves **28**, 969–978 (2007)

[10] A.D. Rakić, T. Taimre, K. Bertling, Y. L. Lim, P. Dean, A. Valavanis, and D. Indjin, “Sensing and imaging using laser feedback interferometry with quantum cascade lasers,” Appl. Phys. Rev. **6**, 021320 (2019).

[11] J. Keeley, K. Bertling, P. L. Rubino, Y. L. Lim, T. Taimre, X. Qi, I. Kundu, L. H. Li, D. Indjin, A. D. Rakić, E. H. Linfield, A. G. Davies, J. Cunningham, and P. Dean, “Detection sensitivity of laser feedback interferometry using a terahertz quantum cascade laser,” Opt. Lett. **44**, 3314–3317 (2019).

[12] K. Bertling, T. Taimre, G. Agnew, Y. L. Lim, P. Dean, D. Indjin, S. Höfling, R. Weih, M. Kamp, M. von Edlinger, J. Koeth, and A. D. Rakić, “Simple electrical modulation scheme for laser feedback imaging,” IEEE J. Sensors **16**, 1937–1942 (2016).

[13] A.D. Rakić, T. Taimre, K. Bertling, Y. L. Lim, P. Dean, D. Indjin, Z. Ikonic, P. Harrison, A. Valavanis, S. P. Khanna, M. Lachab, S. J. Wilson, E. H. Linfield, and A. G. Davies, “Swept-frequency feedback interferometry using terahertz frequency QCLs: a method for imaging and materials analysis,” Opt. Express **21**, 22194–22205 (2013).

[14] S. Han, K. Bertling, P. Dean, J. Keeley, A. D. Burnett, Y. L. Lim, S. P. Khanna, A. Valavanis, D. Indjin, E. H. Linfield, A. G. Davies, T. Taimre, and A. D. Rakić, “Laser feedback interferometry as a tool for analysis of compound mixtures at terahertz frequencies: towards imaging and identification of plastic explosives,” Sensors **16**, 352 (2016).

[15] K. Bertling, S. Han, T. Wu, C. Zhao, Y. L. Lim, P. Dean, S. P. Khanna, D. Indjin, E. H. Linfield, A. G. Davies, S. J. Wilson, T. Taimre, and A. D. Rakić, “Determining ethanol content of liquid solutions using laser feedback interferometry with a terahertz quantum cascade laser,” IEEE Sens. Lett. **2**, 1–4 (2018).

[16] G. Agnew, A. Grier, T. Taimre, K. Bertling, Y. L. Lim, Z. Ikonic, P. Dean, A. Valavanis, D. Indjin, and A. D. Rakić, “Frequency tuning range control in pulsed terahertz quantum-cascade lasers: Applications in interferometry,” IEEE J. Quantum Electron. **54**, 1–8 (2018).

[17] Y. L. Lim, K. Bertling, T. Taimre, T. Gillespie, C. Glenn, A. Robinson, D. Indjin, Y. Han, L. Li, E. H. Linfield, A. G. Davies, P. Dean, and A. D. Rakić, “Coherent imaging using laser feedback interferometry with pulsed-mode terahertz quantum cascade lasers,” Opt. Express **27**, 10221–10233 (2019).

[18] K. Singh, A. Bandyopadhyay, K. Bertling, Y. L. Lim, T. Gillespie, A. Robinson, D. Indjin, Y. Han, L. Li, E. H. Linfield, A. G. Davies, P. Dean, A. D. Rakić, and A. Sengupta, "Monitoring Water Dynamics in Plants using Laser Feedback Interferometry," in 14th Pacific Rim Conference on Lasers and Electro-Optics (CLEO PR 2020), OSA Technical Digest (2020).

[19] M. Wienold, L. Schrottke, M. Giehler, R. Hey, W. Anders, and H. T. Grahn, “Low-voltage terahertz quantum-cascade lasers based on LO-phonon-assisted interminiband transitions,” Electron. Lett. **45**, 1030–1031 (2009).

[20] J. Keeley, J. Freeman, K. Bertling, Y. L. Lim, R. A. Mohandas, T. Taimre, L. H. Li, D. Indjin, A. D. Rakić, E. H. Linfield, A. G. Davies, and D. Paul, “Measurement of the emission spectrum of a semiconductor laser using laser-feedback interferometry,” Sci. reports **7**, 1–9 (2017).